J|A|C|S
COMMUNICATIONS

Published on Web 06/29/2002

Potential Surface for the Quadruply Degenerate Rearrangement of Bicyclo[3.1.0]hex-2-ene

Christopher P. Suhrada and K. N. Houk*

Department of Chemistry and Biochemistry, University of California, Los Angeles, California 90095-1569

Received April 26, 2002

The degenerate rearrangement of bicyclo[3.1.0]hex-2-ene (**1**) to three identical products differing only by the position of a substituent or isotopic label (Scheme 1) has been called "an ideal case for theory-based studies of the behavior of diradical structures launched onto a relatively flat potential surface having alternative exit channels".[1] Three pathways lead to the following products: [1,3] carbon shifts with *retention*, *suprafacial* (1*r*,3*s*) or *inversion*, *antarafacial* (1*i*,3*a*) stereochemistry, and a two-center epimerization (1*i*,1*i*). Labeled and substituted versions of this reaction have been studied,[1−3] and, in all cases, there has been found a nonstatistical ratio of rates (1*r*,3*s*):(1*i*,1*i*):(1*i*,3*a*) in the range from 4:2:2 to 4:3:1. Most recently, Baldwin and Keliher thermolyzed 4-*exo*-*d*-bicyclo-[3.1.0]hex-2-ene (4*x*-**1**) and measured the rates of formation of isotopomeric products 6*x*-**1**, 4*n*-**1**, and 6*n*-**1**, with results shown in Scheme 1.[1]

This reaction is a degenerate case of the vinylcyclopropane−cyclopentene rearrangement, thought to proceed by cleavage of the three-membered ring to form a diradical intermediate.[3] Theoretical findings have fortified and expanded our understanding of the VCP−CP rearrangement as a diradical-mediated process.[4]

In light of the nonstatistical product distribution, and by analogy to the parent VCP, the bicyclo[3.1.0]hex-2-ene autemerization is likely to involve what has been variously called a *twixtyl*,[5] a *continuous diradical*,[6] or a *caldera*.[7] Such species are diradicals that have no deep minima on the potential surface and have a large flat region where geometrical variations result in very small changes in energy. We report DFT, CASSCF, and CASPT2 calculations that detail the potential energy landscape for this reaction and provide a qualitative understanding of the product ratios observed experimentally.

Minima and saddle points were optimized with both (U)B3LYP/6-31G* and (4,4)CASSCF/6-31G* using Gaussian 98.[8] The CASSCF structures are shown in Figure 1. The (4,4)CASPT2/6-31G* single-point energy was calculated in MOLCAS[9] for each CASSCF structure. Zero-point and thermal corrections for 513 K[1] were calculated using (U)B3LYP and CASSCF frequencies. The results are summarized in Table 1, and the CASSCF surface is plotted in Figure 2. A C_S minimum (**1**-C_S) was found for the singlet diradical; the planar structure **1**-C_{2v} was found to be a transition state on the electronic potential surface, but the small energy difference between it and the C_S structure all but vanishes upon inclusion of thermal corrections. **1**-C_S and **1**-C_{2v} are separated from the reactant and products **1** by a small barrier present at the transition structure **1-TS**. At the CASPT2//CASSCF level, the calculated E_a = 41.0 kcal/mol is reasonably close to the experimental value (E_a = 43.8−44.8 kcal/mol).[1]

The structures **1**-C_S, **1**-C_{2v}, and **1-TS** are identified as *diradical* in nature on the basis of a lack of significant interaction between the allyl radical (C1−C2−C3) and the secondary radical (C5), the SOMOs of which have different symmetries. Evidence for this comes from triplet single-point energies calculated on the singlet stationary point geometries. At the CASPT2 level, the triplet state is 0.6−1.3 kcal/mol *lower* in energy than the singlet for **1**-C_S, **1**-C_{2v}, and **1-TS**.

In the thujene (**2**) study, Doering proposed that an "isoconformational" C_S diradical mediates the predominant (1*r*,3*s*) path. C5 begins below the C2−C6−C4 plane as drawn (4*x*-**1**, Figure 2a) and stays below the plane (θ < 180°) in the isoconformational **1**-C_S^i and in the (1*r*,3*s*) product 6*x*-**1**. Moving on the plot from west to east, the isoconformational C_S envelope structure flips via a planar transition state (**1**-C_{2v}) to form the "anticonformational" (θ > 180°)

Scheme 1. Isomerization Pathways Observed with 4*x*-**1**[1] [a]

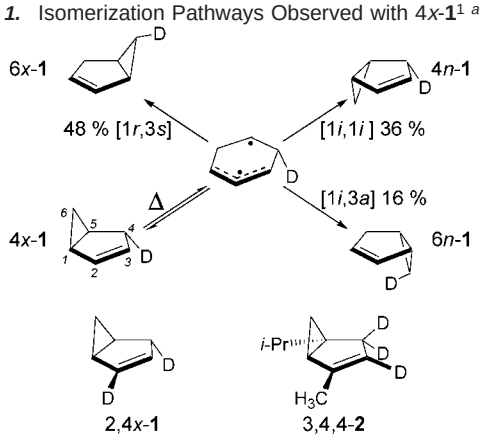

[a] Percentages reflect relative rates for 4*x*-**1**; similar results are found with 6*x*-**1**,[1] 2,4*x*-**1**,[2] and 3,4,4-**2**.[3]

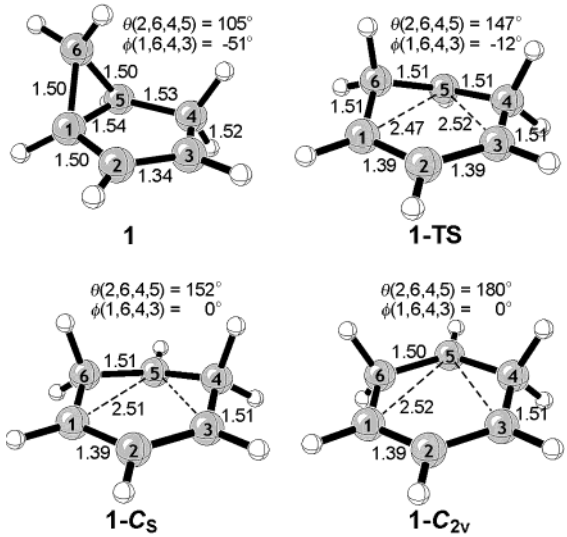

Figure 1. Stationary point structures optimized with (4,4)CASSCF/6-31G*. **1** and **1**-C_S are PES minima; **1-TS** and **1**-C_{2v} are saddle points. Distances are indicated in angstroms.

* To whom correspondence should be addressed. E-mail: houk@chem.ucla.edu.

10.1021/ja020601l CCC: $22.00

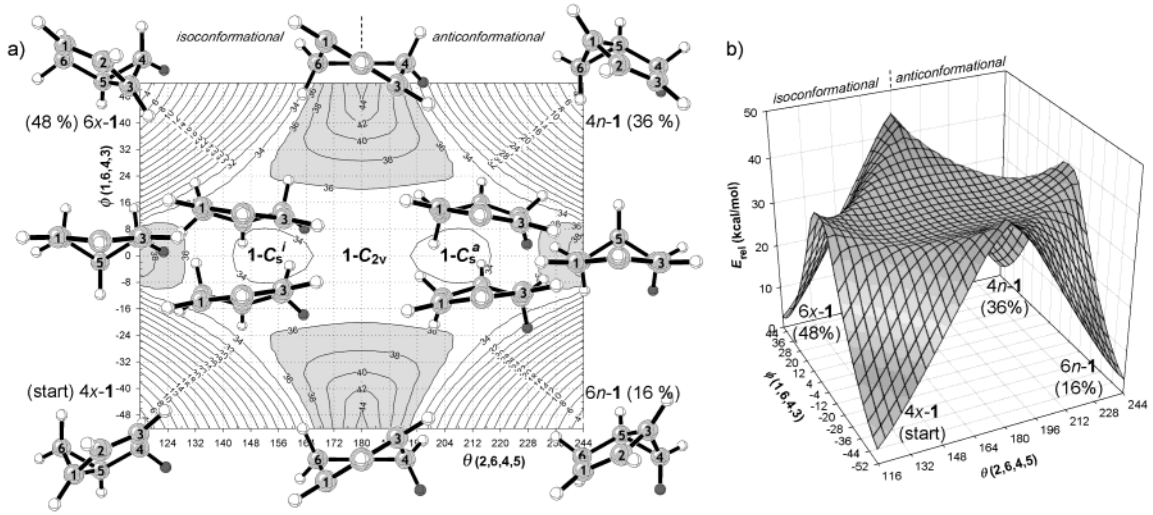

Figure 2. Two views of the (4,4)CASSCF/6-31G* electronic potential energy surface for automerization of **1**. The four structures in the central region of the diagram in (a) are the isoenergetic, isotopomeric **1-TS** structures (E_{rel} = 35.6 kcal/mol; exact positions on plot indicated by the location of C2 atoms).

Table 1. Calculated Relative Enthalpies and Free Energies (kcal/mol at 513 K) of Stationary Points Shown in Figure 1

method		**1**	**1-TS**	**1-C_S**	**1-C_{2v}**
(U)B3LYP/6-31G*	ΔH	0.0	34.6	32.6	32.6
	ΔG	0.0	32.6	30.9	31.6
(4,4)CASSCF/6-31G*	ΔH	0.0	33.1	31.7	31.8
(4,4)CASPT2/6-31G*	ΔH	0.0	40.0	39.9	39.6
	ΔG	0.0	37.8	38.1	37.6

1-C_S^a with C5 above the C2−C6−C4 plane. From here, products 4*n*-**1** and 6*n*-**1** are formed. Recognizing that the C1−C3 axis twists relative to the C4−C6 axis in going from 4*x*-**1** to 6*x*-**1** and from 6*n*-**1** to 4*n*-**1**, we assigned the C1−C6−C4−C3 dihedral (ϕ) to the north−south coordinate. Structures on the equator, including **1-C_S** and **1-C_{2v}**, have a plane of symmetry. Structures along the central meridian, for example, **1-C_{2v}**, have a C_2 axis through C2 and C5. The dihedral parameters we have chosen as coordinates respect the symmetry between reactant and products and correlate well with very low-frequency vibrations[10] calculated for **1-TS**, **1-C_S**, and **1-C_{2v}**.

The barriers separating the intermediates **1-C_S** from one another (**1-C_{2v}**) and from products **1** (**1-TS**) are extremely small or nonexistent. Even if it were possible to define *intermediates* and *transition states* in this *caldera* region with certainty, this situation would not be suitable for the statistical approach of transition state theory. Reactant trajectories have substantial freedom as to how and where they reach, traverse, and exit the transition region. The shaded portion of the plot in Figure 2a includes those points whose energy is more than 0.4 kcal/mol higher than that of **1-TS** at the CASSCF level; the unshaded area represents that large portion of the surface which is easily accessible to molecules that have sufficient energy to react. As reactants enter the transition region, about one-half (48%) continue the clockwise motion of C1−C2−C3 *without* experiencing a C5 envelope flip; these form 6*x*-**1**. The other half (52%) *do* pass through a planar (θ = 180°) structure and enter the anticonformational half of the diradical plateau. While these two paths are clearly not strictly degenerate, there appears to be no major preference for one over the other. Although this is by no means quantitatively predictable from our calculations, analysis of the motions involved in the imaginary frequency of **1-TS** indicates momentum toward both directions. Of the 52% entering the anticonformational region, about two-thirds continue the clockwise C1−C2−C3 motion to form 4*n*-**1**, while the remaining minority reverse this motion to form 6*n*-**1**. This unequal partitioning fits well with Carpenter's *dynamic matching*[11] hypothesis, which is to say that the majority of anticonformational-bound trajectories are inertially predisposed toward 4*n*-**1** upon entering the transition region.

A quantitative test of this tableau, in the form of quasi-classical dynamic trajectory simulations,[11c,12] is currently underway.[13]

Acknowledgment. We thank the National Science Foundation for financial support through a research grant to K.N.H. and an IGERT MCTP fellowship to C.P.S.

Supporting Information Available: Computational procedural details, Cartesian coordinates, and a full citation for MOLCAS 5.0 (PDF). This material is available free of charge via the Internet at http://pubs.acs.org.

References

(1) Baldwin, J. E.; Keliher, E. J. *J. Am. Chem. Soc.* **2002**, *124*, 380.
(2) Cooke, R. S.; Andrews, U. H. *J. Am. Chem. Soc.* **1974**, *96*, 2974.
(3) (a) Doering, W. v. E.; Lambert, J. B. *Tetrahedron* **1963**, *19*, 1989. (b) Doering, W. v. E.; Schmidt, E. K. G. *Tetrahedron* **1971**, *27*, 2005.
(4) (a) Davidson, E. R.; Gajewski, J. J. *J. Am. Chem. Soc.* **1997**, *119*, 10543. (b) Houk, K. N.; Nendel, M.; Wiest, O.; Storer, J. W. *J. Am. Chem. Soc.* **1997**, *119*, 10545. (c) Doubleday, C.; Nendel, M.; Houk, K. N.; Thweatt, D.; Page, M. *J. Am. Chem. Soc.* **1999**, *121*, 4720. (d) Nendel, M.; Sperling, D.; Wiest, O.; Houk, K. N. *J. Org. Chem.* **2000**, *65*, 3259.
(5) Hoffmann, R.; Swaminathan, S.; Odell, B. G.; Gleiter, R. *J. Am. Chem. Soc.* **1970**, *92*, 7091.
(6) Doering, W. v. E.; Sachdev, K. *J. Am. Chem. Soc.* **1974**, *96*, 1168.
(7) Doering, W. v. E.; Ekmanis, J. L.; Belfield, K. D.; Klärner, F.-G.; Krawczyk, B. *J. Am. Chem. Soc.* **2001**, *123*, 5532.
(8) Frisch, M. J.; Trucks, G. W.; Schlegel, H. B.; Scuseria, G. E.; Robb, M. A.; Cheeseman, J. R.; Zakrzewski, V. G.; Montgomery, J. A., Jr.; Stratmann, R. E.; Burant, J. C.; Dapprich, S.; Millam, J. M.; Daniels, A. D.; Kudin, K. N.; Strain, M. C.; Farkas, O.; Tomasi, J.; Barone, V.; Cossi, M.; Cammi, R.; Mennucci, B.; Pomelli, C.; Adamo, C.; Clifford, S.; Ochterski, J.; Petersson, G. A.; Ayala, P. Y.; Cui, Q.; Morokuma, K.; Malick, D. K.; Rabuck, A. D.; Raghavachari, K.; Foresman, J. B.; Cioslowski, J.; Ortiz, J. V.; Stefanov, B. B.; Liu, G.; Liashenko, A.; Piskorz, P.; Komaromi, I.; Gomperts, R.; Martin, R. L.; Fox, D. J.; Keith, T.; Al-Laham, M. A.; Peng, C. Y.; Nanayakkara, A.; Gonzalez, C.; Challacombe, M.; Gill, P. M. W.; Johnson, B. G.; Chen, W.; Wong, M. W.; Andres, J. L.; Head-Gordon, M.; Replogle, E. S.; Pople, J. A. *Gaussian 98*, revision A.9; Gaussian, Inc.: Pittsburgh, PA, 1998.
(9) MOLCAS Version 5.0. See Supporting Information for full citation.
(10) For **1-TS** in CASSCF (unscaled): ν = 113 cm^{-1} corresponds to change in θ (2,6,4,5), and ν = 267 cm^{-1} corresponds to change in ϕ (1,6,4,3).
(11) (a) Carpenter, B. K. *Acc. Chem. Res.* **1992**, *25*, 520. (b) Carpenter, B. K. *J. Am. Chem. Soc.* **1995**, *117*, 6336. (c) Carpenter, B. K. *J. Am. Chem. Soc.* **1996**, *118*, 10329. (d) Carpenter, B. K. *Angew. Chem., Int. Ed.* **1998**, *37*, 3340.
(12) (a) Doubleday, C.; Bolton, K.; Hase, W. L. *J. Am. Chem. Soc.* **1997**, *119*, 5251. (b) Doubleday, C.; Bolton, K.; Hase, W. L. *J. Phys. Chem. A* **1998**, *102*, 3648. (c) Doubleday, C. *J. Phys. Chem. A* **2001**, *105*, 6333.
(13) Collaboration with Charles Doubleday of Columbia University.

JA020601L